Am J Cancer Res 2024;14(7):3335-3347
www.ajcr.us /ISSN:2156-6976/ajcr0157263

Original Article

Engineered exosomes transporting the lncRNA, SVIL-AS1, inhibit the progression of lung cancer via targeting miR-21-5p

Hao Xu, Hongda Ma, Lifen Zha, Qian Li, Huiming Pan, Ladi Zhang

Department of Respiratory, The People's Hospital of Danyang, Affiliated Danyang Hospital of Nantong University, Danyang 212300, Jiangsu, China

Received April 18, 2024; Accepted June 20, 2024; Epub July 15, 2024; Published July 30, 2024

Abstract: In this study, we constructed engineered exosomes carrying the long non-coding RNA (lncRNA) SVIL-AS1 (SVIL-AS1 Exos), and explored its role and mechanism in lung cancer. After the construction of SVIL-AS1 Exos, their physicochemical characteristics were identified. Then, their function and effect in three different cell lines, A549, HeLa, and HepG2, were detected using western blot, the quantitative reverse transcriptase polymerase chain reaction, flow cytometry, 5-ethynyl-2'-deoxyuridine, and Cell Counting Kit-8 experiments. Finally, a mouse xenograft model was constructed to analyze tumor growth and explore the *in vivo* utility of SVIL-AS1 Exos using hematoxylin and eosin staining, immunohistochemistry, and the TdT-mediated dUTP nick end labeling assay. The results demonstrated that SVIL-AS1 Exos preferentially targeted A549 lung cancer cells over HeLa and HepG2 cells. SVIL-AS1 Exos promoted apoptosis and inhibited A549 cell proliferation by elevating expression of the lncRNA, SVIL-AS1. *In vivo*, SVIL-AS1 Exos effectively inhibited the growth of lung cancer A549 cells. Furthermore, SVIL-AS1 Exos suppressed the expression of miR-21-5p and upregulated the expression of caspase-9, indicating that SVIL-AS1 may regulate the development of lung cancer through the miR-21-5p/caspase-9 pathway. In conclusion, the engineered SVIL-AS1 Exos targeted lung cancer cells to inhibit the expression of miR-21-5p, upregulate the expression of caspase-9, and inhibit the development of lung cancer.

Keywords: Engineered exosomes, LncRNA SVIL-AS1, lung cancer, miR-21-5p

Introduction

Lung cancer is one of the most common malignancies, and the most prevalent cause of cancer-related deaths around the world [1-4]. According to the Global Assessment Model of Cancer in 2023, lung cancer ranked first in terms of mortality, accounting for 20.8% of all cancer cases [5]. Although prompt interventions, such as radiation, surgery, and chemotherapy, have improved clinical outcomes and overall survival, lung cancer mortality rates remain significantly high [5].

Long non-coding RNAs (lncRNAs), a class of mature RNAs that do not encode proteins, play critical roles in cancer development [6]. The significance of lncRNAs in the progression of lung cancer has been the subject of extensive research, revealing that numerous lncRNAs have unique expression patterns, molecular targets, and functional processes [7, 8]. For instance, the lncRNA, JPX, influences lung cancer development and metastasis by triggering Wnt/β-catenin signaling [9]. LncRNA H19 facilitates the growth and spread of lung cancer [10]. LncRNA MALAT1 contributes to gefitinib resistance and lung cancer growth [11]. Lung cancer-associated transcript 1, a novel lncRNA, functions as an oncogene in the progression of lung cancer [12]. The lncRNA, u50535, accelerates lung cancer growth by triggering CCL20/extracellular signal-regulated kinase signaling [13]. Research by Acha-Sagredo et al. [14] noted that the lncRNA, SVIL-AS1, is significantly downregulated in non-small cell lung cancer (NSCLC) and is associated with tumor stage, showing lower expression in stage T1 compared to T3 NSCLC tumors. Hu et al. [15] found that SVIL-AS1 was downregulated in lung adenocar-

https://doi.org/10.62347/YRJK5888

cinoma tissues and correlated with a good prognosis in such patients, whereas overexpression of SVIL-AS1 inhibited lung adenocarcinoma cell proliferation. However, these studies have not extensively explored how SVIL-AS1 influences the onset and progression of lung cancer.

Exosomes are small membrane vesicles, ranging from 30 to 150 nm in diameter. They are released by parental cells into the extracellular milieu and play a role in several biological activities [16-18]. Exosomes may act as channels for cell-cell communication *in vivo* by effectively delivering functional mRNAs, micro RNAs (miRNAs), lncRNAs, circular RNAs, and proteins to recipient cells, thereby influencing cancer progression [19-22]. Therefore, utilizing modified exosomes to deliver therapeutic nucleic acids to certain tumor cells is a promising approach for developing efficient anticancer therapies [23-25].

In this study, we constructed exosomes carrying the lncRNA, SVIL-AS1, and detected their uptake by A549 cells. To reveal the underlying processes, we screened the downstream targets of SVIL-AS1 using bioinformatics and verified them using cell experiments.

Materials and methods

Analysis of cancer-omics data

The expression levels of lncRNAs and miRNAs in lung adenocarcinoma and squamous cell carcinoma were analyzed using the Gene Expression Profiling Interactive Analysis (GEPIA) (http://gepia2.cancer-pku.cn/#index) and UALCAN (https://ualcan.path.uab.edu/analysis.html) databases. Interactions between lncRNAs and miRNAs were examined using DIANA (https://diana.e-ce.uth.gr/lncbasev3/interactions) and the miRWalk database (http://mirwalk.umm.uni-heidelberg.de/).

Cell culture

The 293T, A549, HeLa, and HepG2 cell lines were acquired from the Cell Resource Center of the Shanghai Academy of Sciences. 293T, HeLa, and HepG2 cells were cultured in Dulbecco's modified Eagle's medium, whereas A549 cells were grown in RPMI-1640 medium. Both media were supplemented with 10% fetal bovine serum (10099158; Gibco, Grand Island, NY, USA) and 1% penicillin-streptomycin. All cell lines were maintained at 37°C in an atmosphere containing 5% CO_2.

Engineered exosome preparation

The pcDNA 3.1 plasmid (V79020, Invitrogen, Carlsbad, CA, USA) was engineered to exclusively express SVIL-AS1 and was transfected into 293T cells. Exosomes were isolated from these cells using a series of density gradient ultracentrifugation steps. Briefly, 293T cell culture medium was subjected to successive centrifugation at 1000 × g for 15 min, 3000 × g for 25 min, 6000 × g for 40 min, and 10,000 × g for 1 h. The supernatants were collected after each step. Then, the collected supernatants were ultracentrifuged at 100,000 × g for 70 min at 4°C. The resulting pellet containing the exosomes was washed with phosphate-buffered saline (PBS) and centrifuged again under the same conditions to obtain a purified exosome pellet.

Transmission electron microscopy (TEM)

The exosome pellets were fixed with 2.5% glutaraldehyde at 4°C, dehydrated in progressively higher concentrations of ethanol, then visualized using TEM (JEM-F200, JEOL, Tokyo, Japan) at 80 kV.

Detection of PKH26-labeled SVIL-AS1 exosomes (SVIL-AS1 Exos)

SVIL-AS1 Exos were labeled with the PKH26 dye in strict accordance with the instructions of the PKH26 Fluorescent Cell Ligation Kit (MINI26-1KT; Sigma-Aldrich, St. Louis, MO, USA). After labeling, the exosomes were washed to remove excess dye. A549, HeLa, and HepG2 cells were seeded in dishes for confocal microscopy. Once the cells reached an appropriate density, they were incubated with labeled SVIL-AS1 Exos. At predetermined time points, the cells were washed with PBS to remove non-absorbed exosomes, and the nuclei were labeled with Hoechst 33258 (94403, Sigma-Aldrich) for 15 min at room temperature. After washing with PBS, images of the red (PKH26-labeled exosomes) and blue (Hoechst 33258-labeled nuclei) channels were taken separately using a TCS SP8 X confocal microscope (Leica, Wetzlar, Germany).

Western blot assay

Cells and exosomes were lysed for 15 min using radioimmunoprecipitation assay lysis buffer (R0020; Solarbio, Shanghai, China) containing 0.5% phenylmethanesulfonyl fluoride. Total protein was measured using a BCA Protein Assay Kit (23225, Thermo Scientific, Waltham, MA, USA). Proteins were separated by electrophoresis and transferred onto membranes that were then blocked with bovine serum albumin (37525, Thermo Scientific) at room temperature for 30 min. The membranes were incubated overnight at 4°C with primary antibodies, and for 1 h at room temperature with secondary antibodies. The primary antibodies were: anti-CD63 (1:1000 dilution, ab134045), anti-CD9 (1:1000 dilution, ab236630), anti-calnexin (1:1000 dilution, ab22595), anti-caspase-9 (1:500 dilution, ab32539), anti-Bax (1:1000 dilution, ab32503), anti-Bcl-2 (1:1000 dilution, ab182858), anti-cleaved-caspase-3 (1:500 dilution, ab32042), anti-cleaved-caspase-9 (1:500 dilution, 9509), and anti-β-actin (1:5000 dilution, ab8226). Horseradish peroxidase-labeled goat anti-rabbit (1:5000 dilution, ab216773) and goat anti-mouse (1:5000 dilution, ab175783) were used as secondary antibodies. All antibodies were from Abcam (Cambridge, MA, USA) except anti-cleaved-caspase-9 from Cell Signaling Technology (Danvers, MA, USA). Protein bands were visualized using an enhanced chemiluminescence kit (E412-01/02, Vazyme, Nanjing, China) and quantified using ImageJ software (National Institutes of Health, Bethesda, MD, USA).

Cell viability assay

The viability of A549, HeLa, and HepG2 cells exposed to PBS, normal unloaded exosomes (Exos), non-cargo (NC) Exos, or SVIL-AS1 Exos was assessed using the Cell Counting Kit-8 (CCK8) test. A549, HeLa, and HepG2 cells were seeded into 96-well plates containing 10% fetal calf serum at a density of 1×10^4 cells/well. After 0, 24, 48, and 72 h of treatment, 10 μL/well of CCK8 reagent (CKD4-1000T, Doujindo, Kumamoto, Japan) were added per well. After incubation at 37°C for 45 min, cell viability was analyzed by measuring the optical density values using a SpectraMax M2 automated microplate reader at 450 nm (Molecular Devices, Sunnyvale, CA, USA).

Ethynyl-2'-deoxyuridine (EdU) incorporation assay

The proliferation of A549 cells treated with PBS, Exos, NC Exos, or SVIL-AS1 Exos was evaluated using the Click-iT® EdU Alexa Fluor® Imaging Kit (C10339, Invitrogen). After treatment, the cells were incubated with EdU-containing medium for 2 h and washed twice with PBS. Cells were permeabilized with 0.5% Triton X-100 and fixed with 4% paraformaldehyde. Nuclei were counterstained with Hoechst 33258 (H1398, Invitrogen) for 15 min. The percentage of EdU-positive cells was determined under a TI-S fluorescence microscope (Nikon, Tokyo, Japan) to assess cell proliferation in various treatment groups.

Cell apoptosis analysis

The proportion of apoptotic cells was determined using flow cytometry. A549 cells (1×10^5) were treated with PBS, Exos, NC Exos, or SVIL-AS1 Exos, collected, suspended in 100 μL combining buffer, and then incubated while protected from light with 5 μL Annexin V-FITC and 5 μL propidium iodide staining solution from the Annexin V-FITC/PI Apoptosis Detection Kit (A214-01, Vazyme) for 10 min at room temperature. Stained cells were then diluted in 400 μL of combining buffer and analzyed by flow cytometry (Leica), with data processed using FlowJo 10 software.

RNA extraction and the quantitative real-time polymerase chain reaction (qRT-PCR)

Total RNA was extracted from A549 cells treated with PBS, Exos, NC Exos, or SVIL-AS1 Exos, and from the lungs of immunodeficient nude mice injected with these substances, using TRIzol reagent (15596018CN, Invitrogen). In accordance with the manufacturer's instructions for the HiScript II 1st Strand cDNA Synthesis Kit (R223-01, HiScript® II Q RT SuperMix for qPCR, Vazyme), 1 μg of total RNA was reverse transcribed into cDNA. qRT-PCR was performed using ChamQ SYBR qPCR Master Mix (Q311-02, Vazyme) on an ABI 7500 FAST Real-time PCR apparatus (Applied Biosystems, Darmstadt, Germany). Expression levels of SVIL-AS1 were normalized to the housekeeping gene, β-actin. The primers used for β-actin, caspase-9, and SVIL-AS1 are listed in **Table 1**.

Table 1. Primers were adopted for qRT-PCR

Gene name	Forward primer (5'-3')	Reverse primer (5'-3')
β-actin	GGAAATCGTGCGTGACATT	CAGGCAGCTCGTAGCTCTT
LncRNA SVIL-AS1	GCAACAATAGGTGGTCCAC	AAACAAAGGGACTGCTGTC
CASP9	CGAACTAACAGGCAAGCA	CAAATCCTCCAGAACCAAT

Mouse xenograft model

Six-week-old nude mice were purchased from Gem Pharmatech (Nanjing, China). Briefly, the left flank of each mouse was injected subcutaneously with 1×10^6 A549 cells to establish a xenograft model. After cell injection, the mice were administered PBS, Exos, NC Exos, or SVIL-AS1 Exos via tail vein injection. Every seven days, tumor volumes in the NC and SVIL-AS1 groups were assessed. On day 35, the mice were euthanized by cervical dislocation after carbon dioxide asphyxia, and the tumors were removed to examine their size and weight. All animal experiments complied with the local guidelines of Nantong University (IACUC20230304-113) for the care and use of laboratory animals.

Hematoxylin & eosin (HE) staining

All tumor tissues from the NC Exo and SVIL-AS1 Exo mice were fixed in 4% paraformaldehyde for 24 h. Hematoxylin was used to stain the nucleus of the dewaxed sections for 10 min, followed by 30 sec of 1% ethanol-hydrochloric acid and five min of eosin solution, per the HE procedure. The sections were dehydrated in a graded ethanol series and cleared with xylene. Representative images were captured using a TS2 microscope (Nikon, Tokyo, Japan).

Immunohistochemistry (IHC) staining

Deparaffinized tissue samples from the NC and SVIL-AS1 Exo groups were rehydrated using a gradient of ethanol and xylene. Following treatment with a goat anti-rabbit horseradish peroxidase antibody (1:2000 dilution, ab6721, Abcam) for 2 h, the samples were incubated with the primary Ki67 antibody (1:500, ab15580, Abcam) overnight at 4°C. The slices were stained with hematoxylin and diaminobenzidine (D12384, Sigma-Aldrich). Blue particles indicated hematoxylin-stained nuclei, whereas brown-yellow particles reflected Ki67-positive expression.

Terminal deoxynucleoitidyl transferase dUTP nick end labeling (TUNEL) staining

Tissue slices from the SVIL-AS1 Exo and NC Exo groups were embedded in paraffin for 24 h, fixed with 4% paraformaldehyde, and stained using an in situ cell death detection kit (11684817910; Roche, Basel, Switzerland). TUNEL staining was observed under a TS2 microscope, and the proportion of apoptotic cells was evaluated.

Statistical analyses

All data were gathered from three separate tests and are presented as means ± standard deviation. Prism 8.0 software (GraphPad, La Jolla, CA, USA) was adopted to analyze the data. The Shapiro-Wilk test was used to test the normality of all data, and a one-way analysis of variance and the least significant difference method were used for multiple comparisons. $P<0.05$ was considered statistically significant.

Results

Preparation and identification for the engineered unloaded Exos and SVIL-AS1 Exos

TEM and dynamic light scattering were used to distinguish between unloaded Exos and SVIL-AS1 Exos. As shown in **Figure 1A** and **1B**, both unloaded Exos and SVIL-AS1 Exos were solid particles with a typical two-layer membrane structure with an average diameter of 100 nm. The unloaded and SVIL-AS1 Exos exhibited significantly higher protein levels of the exosomal markers CD63 and CD9 compared to the cells, as shown by the western blot analyses (**Figure 1C**). In addition, modified SVIL-AS1 exos were effectively produced, as indicated by the absence of calnexin protein expression in the exosomes, whereas it was present in the cell samples.

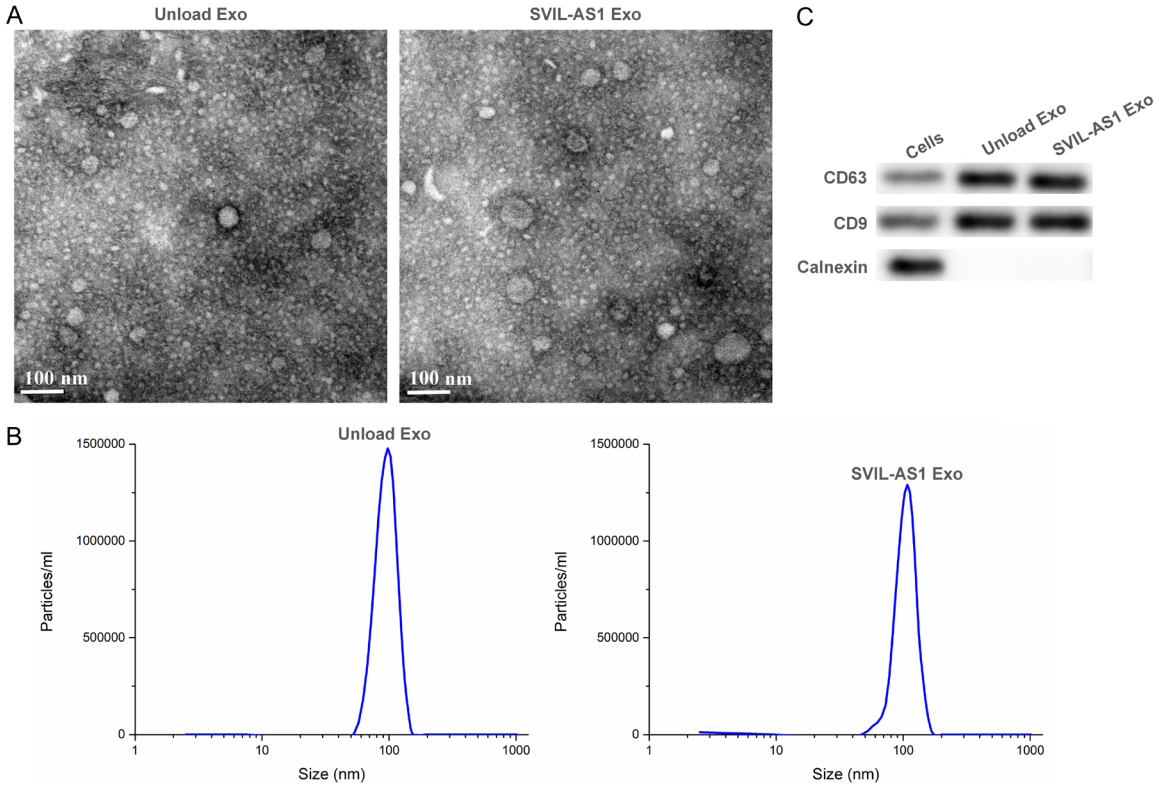

Figure 1. The engineered unload Exo and SVIL-AS1 Exo were obtained and identified. A. The structures of SVIL-AS1 Exo and engineered unload Exo identified by transmission electron microscope. B. The size of SVIL-AS1 Exo and unload Exo was observed using dynamic light scattering. C. Exosome and cell lysis protein levels of exosomal markers (CD63 and CD9) and negative control (calnexin) were examined by Western blot.

Specific uptake of engineered SVIL-AS1 exos by A549 cells

A549, HeLa, and HepG2 cells were co-cultured with PKH26-labeled SVIL-AS1 exos for 48 h. Observation under a fluorescence microscope showed that A549 cells displayed strong red fluorescence, indicating a higher uptake of SVIL-AS1 exosomes compared to HeLa and HepG2 cells ($P<0.05$ and $P<0.001$, respectively) (**Figure 2A**). Additionally, the flow cytometry analysis after a 48 h co-culture revealed an increase in the exosomal surface antigen, CD63, across all cell types (**Figure 2B**). However, this increase was significantly more pronounced in A549 cells than in HeLa or HepG2 cells, confirming the preferential uptake of SVIL-AS1 exos by A549 cells.

SVIL-AS1 Exos promoted caspase-9 expression in A549 cells

Using the GEPIA database, we found that SVIL-AS1 and caspase-9 were expressed at low levels in lung adenocarcinoma and lung squamous cell carcinoma (**Figure 3A**, **3B**). In addition, the UALCAN database revealed that miR-21-5p was highly expressed in lung adenocarcinoma and lung squamous cell carcinoma (**Figure 3C**). The relative expression of SVIL-AS1 in the PBS, unloaded Exo, NC Exo, and SVIL-AS1 Exo groups was examined by qRT-PCR to assess delivery efficiency. **Figure 4A** shows that SVIL-AS1 and caspase-9 expression was upregulated in the SVIL-AS1 Exo group compared to the PBS, unloaded Exo, and NC Exo groups. Western blotting (**Figure 4B**) revealed that the caspase-9 protein level in the SVIL-AS1 Exo group was higher than those in the other three groups, with no changes in the endoplasmic reticulum protein, calnexin.

The link between SVIL-AS1 and caspase-9 was further demonstrated using DIANA (**Figure 3D**) and miRWalk (**Figure 3E**), which revealed an interaction between miR-21-5p and caspase-9. The qRT-PCR results showed that the expression level of miR-21-5p was significantly increased in A549 cells transfected with the miR-21-5p mimic (**Figure 3F**). A549 cells trans-

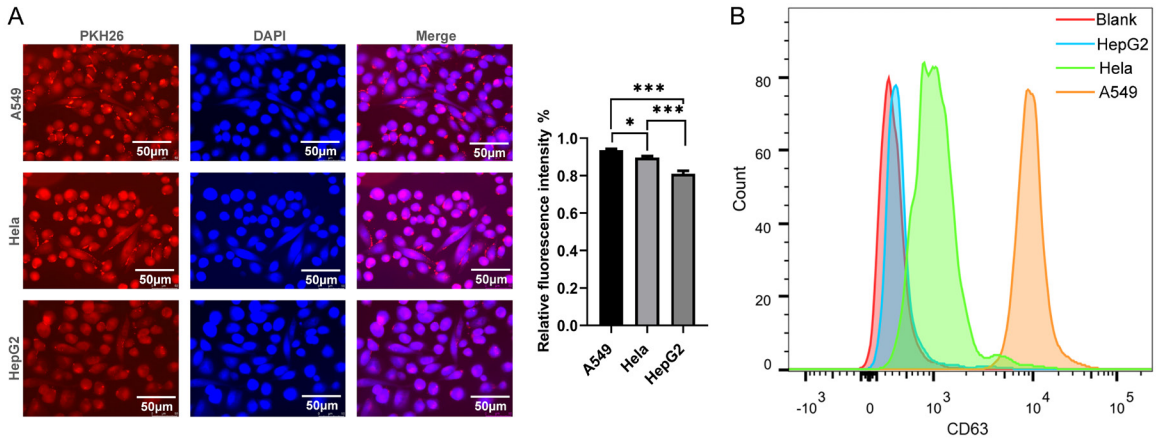

Figure 2. A549 cells could specifically uptake SVIL-AS1 Exo. A. Fluorescence levels in A549, Hela, or HepG2 cells co-cultured with PKH26-labeled SVIL-AS1 exosomes. B. The contents of CD63, a unique marker of exosomes, in A549, Hela, or HepG2 cells treated with PKH26-labeled SVIL-AS1 exosomes (flow cytometry).

fected with wild-type SVIL-AS1 or caspase-9 and the miR-21-5p mimic showed a substantial reduction in luciferase activity, according to a luciferase reporter assay. However, when the putative binding sites in SVIL-AS1 or caspase-9 were altered, there was no discernible variation in luciferase activity (**Figure 3G**, **3H**).

The expression level of SVIL-AS1 in A549 cells transfected with pc-SVIL-AS1 significantly increased (**Figure 3I**), whereas the expression level of miR-21-5p significantly decreased (**Figure 3J**). The qRT-PCR and western blot assays were used to investigate the effect of miR-21-5p overexpression on caspase-9 expression. As demonstrated in **Figure 3K** and **3L**, the mRNA and protein levels of caspase-9 were considerably decreased when miR-21-5p was overexpressed, indicating that the lncRNA, SVIL-AS1, may regulate caspase-9 expression through miR-21-5p.

Effect of SVIL-AS1 Exos on the proliferation of A549, HeLa, and HepG2 cells

CCK8 (**Figure 5A**) and EdU (**Figure 5B**) assays were conducted to identify the effect of PBS, unloaded Exos, NC Exos, or SVIL-AS1 Exos on the proliferation of A549, HeLa, and HepG2 cells. A549 cells co-cultured with SVIL-AS1 Exos showed substantial growth suppression at 24, 48, and 72 h compared to the PBS, unloaded Exos, or NC Exos groups. However, there was no discernible difference in the viability of control and exo-treated HeLa and HepG2 cells (**Figure 5A**). Furthermore, a reduced percentage of EdU-positive proliferating A549 cells was observed in the SVIL-AS1 Exo group, highlighting the role of exosomes in suppressing A549 cell proliferation (**Figure 5B**).

Role of SVIL-AS1 Exos in A549 cell apoptosis

The flow cytometry analysis (**Figure 6A**) revealed a significantly higher percentage of apoptotic A549 cells after treatment with SVIL-AS1 Exos than after treatment with PBS, unloaded Exos, or NC Exos ($P<0.0001$). Western blot assays further supported this finding (**Figure 6B**); treatment with SVIL-AS1 Exos led to increased expression of the pro-apoptotic proteins Bax and cleaved caspases 3 and 9, while expression of the anti-apoptotic protein, Bcl-2, was diminished. These results confirmed that SVIL-AS1 Exos effectively induced apoptosis in A549 cells.

The delivery efficiency of SVIL-AS1 in vivo

To evaluate the in vivo delivery of SVIL-AS1 via exosomes, we assessed whether exosomal SVIL-AS1 altered the expression levels of both SVIL-AS1 and caspase-9 using qRT-PCR and western blotting. Compared to the PBS, unloaded Exo, and NC Exo groups, the SVIL-AS1 Exo group exhibited a significantly higher expression of SVIL-AS1 (**Figure 7A**). Furthermore, the SVIL-AS1 exos group also had increased protein and mRNA expression levels of caspase-9 (**Figure 7B**). These results confirm that SVIL-AS1 was effectively delivered *in vivo*.

Enforced expression of SVIL-AS1 affected lung cancer cell tumorigenicity in vivo

SVIL-AS1 overexpression considerably inhibited A549 cell tumor development *in vivo* (**Figure**

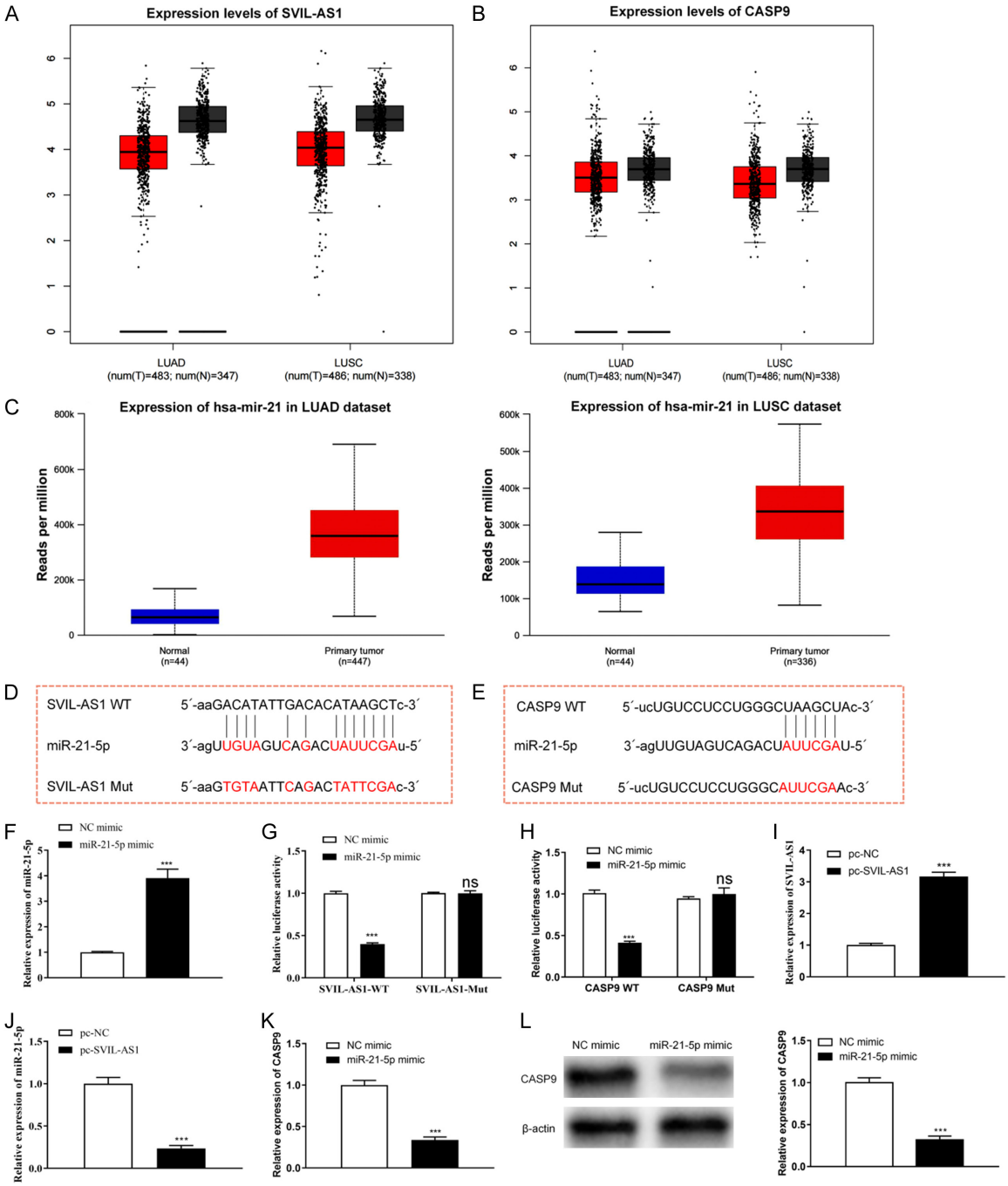

Figure 3. The expression levels of SVIL-AS1 (A) and CASP9 (B) in lung adenocarcinoma and lung squamous cell carcinoma analyzed using GEPIA database. (C) The expression levels of miR-21-5p in lung adenocarcinoma and lung squamous cell carcinoma analyzed by the UALCAN database. (D) The putative combining sites of miR-21-5p for lncRNA SVIL-AS1 predicted by DIANA. (E) The predicted combining sites between miR-21-5p and CASP9. (F) The mRNA levels of miR-21-5p in A549 cells transfected with NC mimics and miR-21-5p mimics were analyzed by qRT-PCR. Luciferase activity assays were adopted to determine the relationship between miR-21-5p and (G) SVIL-AS1 and (H) CASP9. The mRNA levels of SVIL-AS1 (I) and miR-21-5p (J) in A549 cells transfected with pc-NC and pc-SVIL-AS1 were analyzed by qRT-PCR. (K) The mRNA levels of CASP9 in A549 cells transfected with NC mimics and miR-21-5p mimics were analyzed by qRT-PCR. (L) The CASP9 protein expression was detected by Western blot in A549 cells transfected with NC mimics and miR-21-5p mimics. Vs NC mimic or pc-NC, $^{ns}P>0.05$, $^{***}P<0.001$.

8A). The tumor volume and weight in the SVIL-AS1 group were lower than those in the NC Exo group (**Figure 8B**, **8C**). A histopathological analysis using HE staining indicated considerably

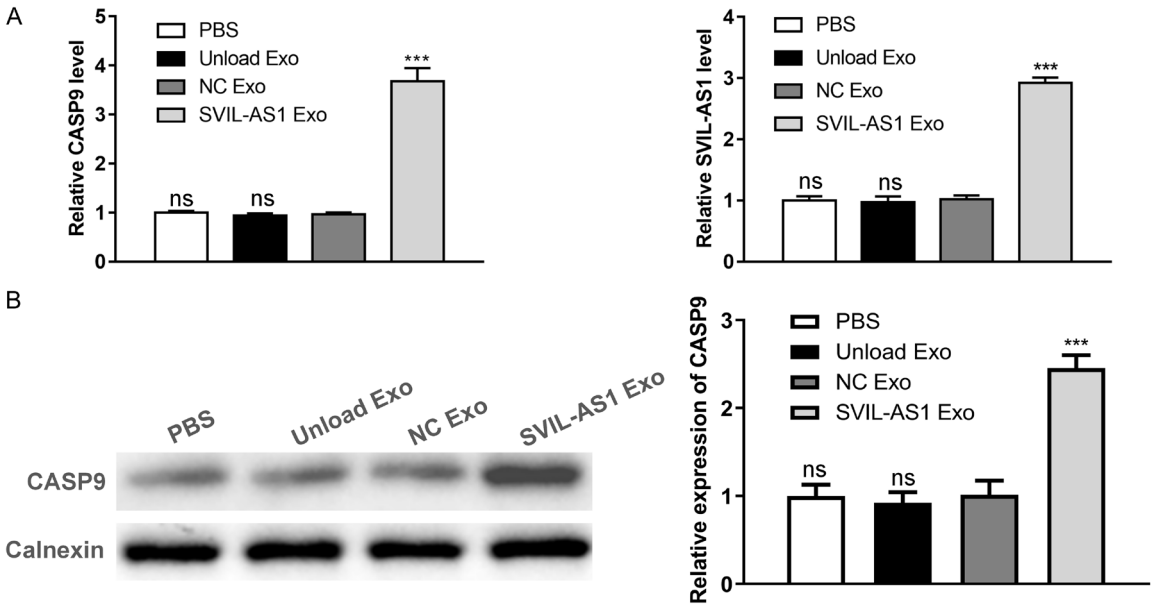

Figure 4. SVIL-AS1 Exo promoted CASP9 expression in A549 cells. A. The mRNA expression of SVIL-AS1 and CASP9 in PBS, unload Exo, NC Exo as well as SVIL-AS1 Exo groups analyzed by qRT-PCR. B. The protein expression of CASP9 in PBS, unload Exo, NC Exo and SVIL-AS1 Exo groups detected by Western blot assay. Vs NC Exo, $^{ns}P>0.05$, $^{***}P<0.001$.

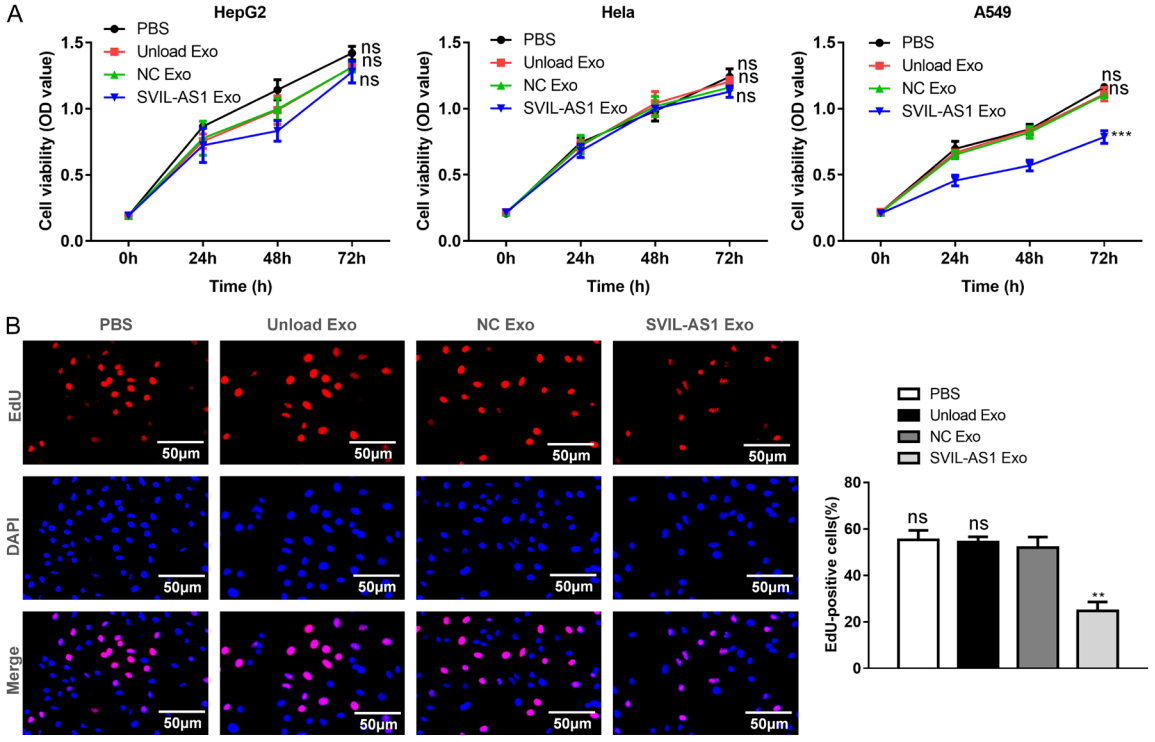

Figure 5. SVIL-AS1 exosomes inhibited the proliferation of A549 cells. A. The proliferation abilities of A549, Hela, or HepG2 cells in PBS, unload Exo, NC Exo and SVIL-AS1 Exo groups were checked by CCK8 assay. B. The cell proliferation of A549 in PBS, unloaded Exo, NC Exo and SVIL-AS1 Exo groups was measured using EdU assay. Vs NC Exo, $^{ns}P>0.05$, $^{**}P<0.01$, $^{***}P<0.001$.

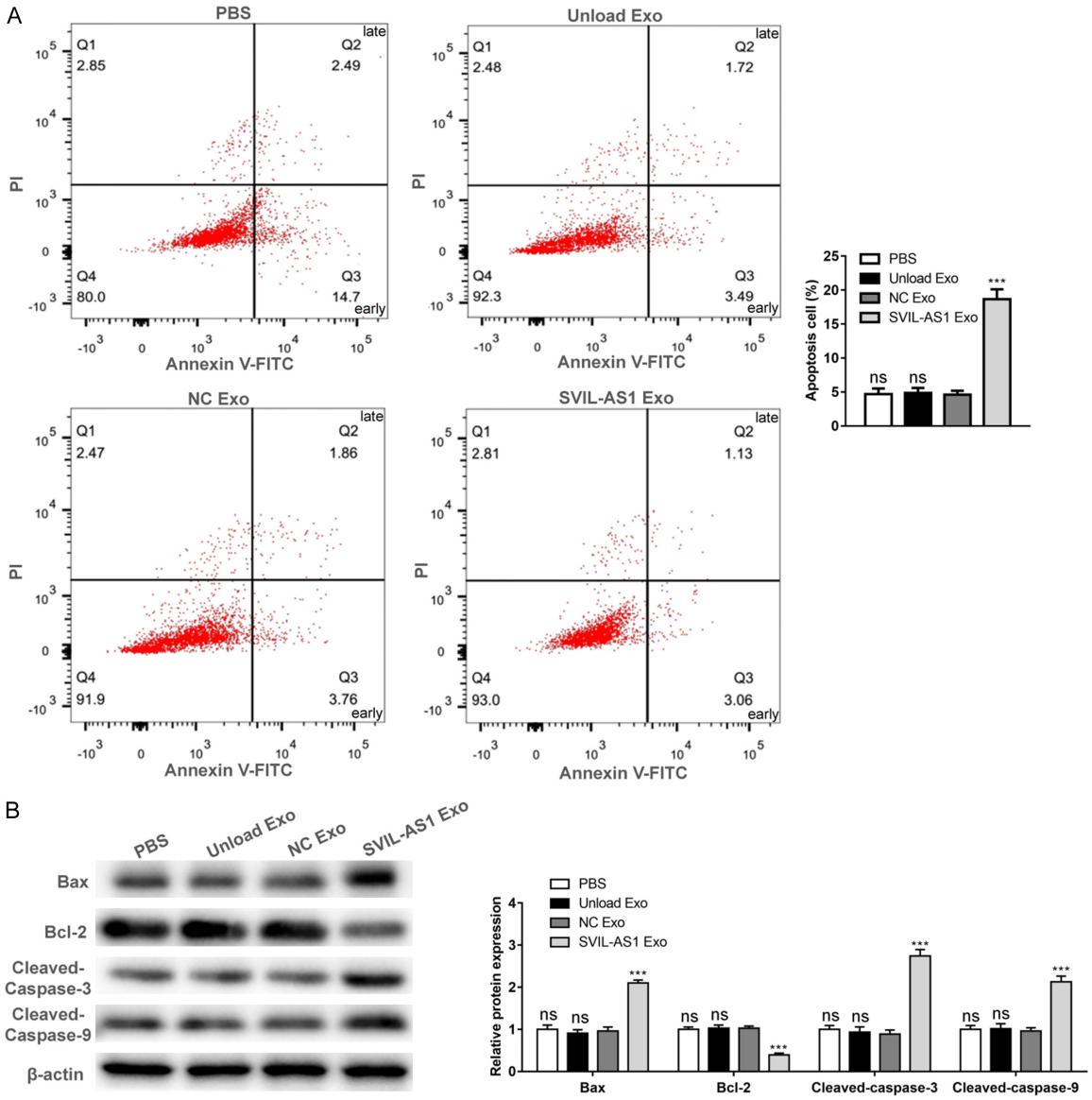

Figure 6. SVIL-AS1 exosomes promoted cell apoptosis for A549 cells. A. The cell apoptosis in A549 cells of various group that detected by Flow cytometry (Q2 represents late apoptosis and Q3 represents early apoptosis). B. The expression levels of apoptosis-related proteins (Bax, cleaved-caspase 3, and cleaved-caspase 9) and anti-apoptosis protein (Bcl-2) in A549 cells of various group that detected by western blot. Vs NC Exo, $^{ns}P>0.05$, $***P<0.001$.

less tumor tissue in the SVIL-AS1 group than in the NC Exo group. Immunohistochemical staining for the proliferation marker Ki67 revealed reduced expression in the SVIL-AS1 group compared to the NC Exo group. Additionally, a higher level of apoptosis was observed in the SVIL-AS1 group as evidenced by TUNEL staining (**Figure 8D**). These findings demonstrated that SVIL-AS1 acts as a tumor suppressor by inhibiting the growth of lung cancer cells *in vivo*.

Discussion

The results of this study showed that SVIL-AS1 Exos were not only efficiently absorbed by A549 lung cancer cells, but also effectively inhibited the growth of these cells in a xenotransplant animal model. These results align with previous research showing that exosomes, due to their high stability and low immunogenicity, can transport various biomolecules such as proteins, miRNA, circular RNA, lncRNA, or mRNA

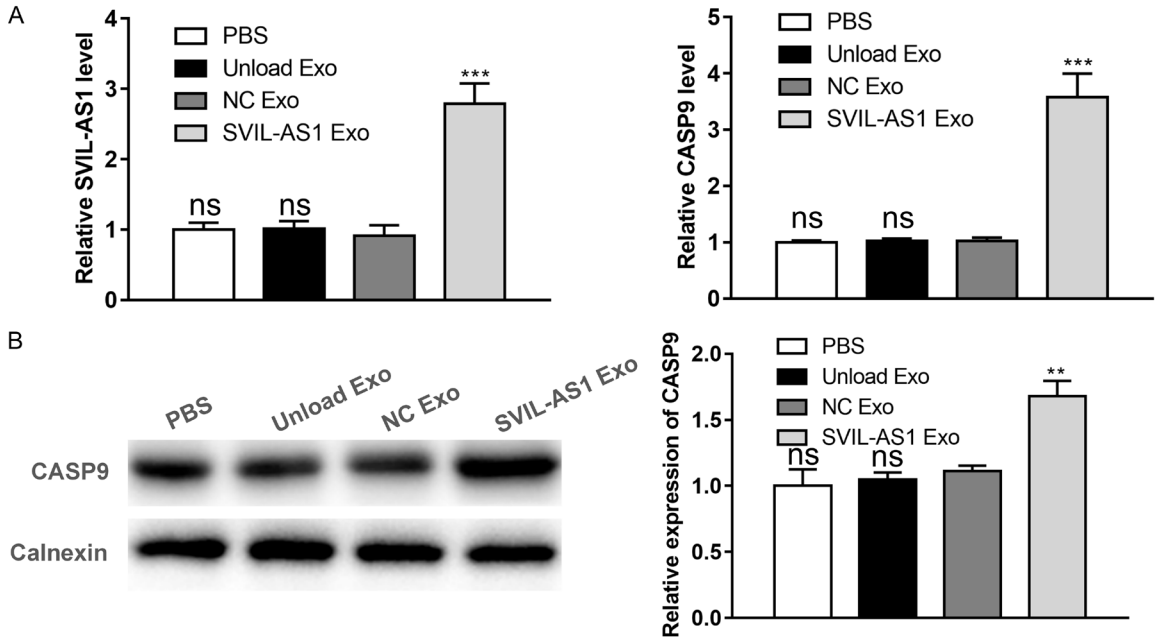

Figure 7. Exosome-mediated delivery of SVIL-AS1 *in vivo* was efficiency. A. The mRNA expression of SVIL-AS1 and CASP9 in the xenograft tissues of mice was detected by qRT-PCR. B. The protein expression of CASP9 in the xenograft tissues of mice was detected by Western blot. Vs NC Exo, $^{ns}P>0.05$, $^{**}P<0.01$, $^{***}P<0.001$.

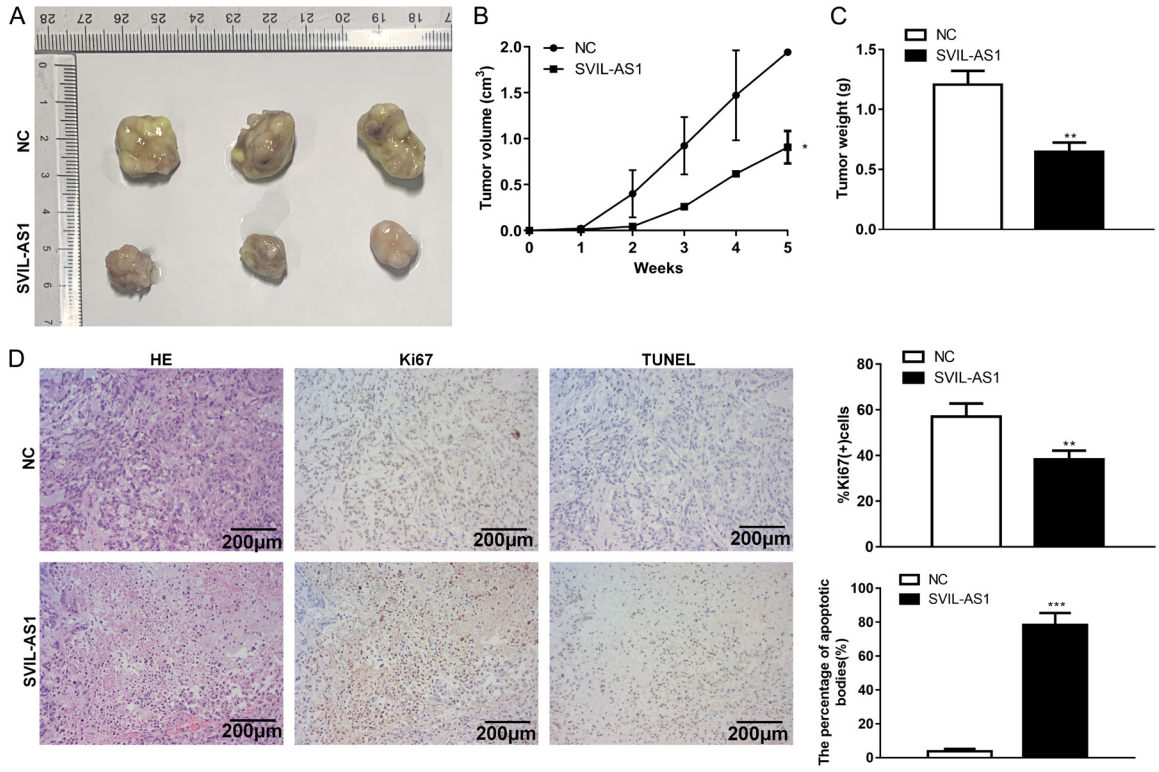

Figure 8. SVIL-AS1 overexpression inhibited tumorigenicity of lung cancer *in vivo*. A. The resected tumors on Day 35. B. The tumor volume that measured every 7 days. C. The tumor weights measured on Day 35. D. The percentage of Ki67-positive cells (HE staining), and tunel staining of tumor tissues in the NC and SVIL-AS1 groups. Vs NC, $^{*}P<0.05$, $^{**}P<0.01$, $^{***}P<0.001$.

into target cells, alter gene expression, and participate in biological processes [26-28]. Moreover, engineered exosomes can successfully deliver exogenous nucleic acids, peptides, or therapeutic drugs to specific cells, particularly cancer cells, making them attractive nanocarriers [29-34].

Some studies have shown that exosomes derived from specific cells can target analogous cells and promote their retention in these cells [35]. For example, Bai et al. [36] found that exosomes targeting the transmembrane peptide, tLyp-1, had high transfection efficiency, while Nie et al. [37] found that miRNA-126 loaded into 231-Exos could recognize A549 cells in the blood and successfully evade the immune surveillance system of NSCLC. Therefore, lung cancer cells along with *in vivo* imaging technology were utilized in our study to detect the targeting efficiency of SVIL-AS1 Exos and improve the precise treatment of lung cancer with these exosomes.

In the current study, expression of the lncRNA, SVIL-AS1, was downregulated in A549 cells, and overexpression of this lncRNA effectively reduced cell viability and promoted cell apoptosis. Previous studies have consistently shown that the expression of SVIL-AS1 is downregulated in cisplatin-resistant lung adenocarcinoma cells, and its overexpression can inhibit the proliferation and cisplatin resistance of these cells [38]. Therefore, SVIL-AS1 may be a potent inhibitor of lung cancer progression. However, because only A549 cells were used in this study, this conclusion needs to be verified using additional cell lines.

The current study found that SVIL-AS1 Exos increased the expression level of SVIL-AS1 in cells and tissues, and upregulated the expression level of caspase-9 by adsorbing miR-21-5p. A previous study showed that SVIL-AS1 overexpression could adsorb MiR-103a and directly target ICE1 to inhibit the proliferation and cisplatin resistance of lung adenocarcinoma cells [38]. However, the mechanism by which SVIL-AS1 regulates the development of lung cancer and participates in cisplatin resistance requires further investigation. Based on the luciferase reporter assay performed in this study, the regulatory mechanism by which SVIL-AS1 adsorbs miR-21-5p and upregulates caspase-9 requires further confirmation by rescue experiments.

Conclusion

In this study, we constructed exosomes carrying the lncRNA, SVIL-AS1, termed SVIL-AS1 Exos, and examined their anticancer potential and target effects. The results showed that SVIL-AS1 Exos effectively delivered SVIL-AS1 *in vitro* and *in vivo* to suppress the progression of lung cancer, indicating that SVIL-AS1 represents a novel avenue for lung cancer therapy. However, validation of the effectiveness of SVIL-AS1 Exos in this study was limited to an intermediate stage between cellular and animal models. The direct detection and comparison of SVIL-AS1 and its targets in exosomes and cells are essential to confirm these findings. Additionally, incorporating experimental studies with other SVIL-AS1 targets is necessary to further establish its specificity in targeting caspase-9 in A549 cells. To underscore the benefits of exosome-mediated delivery, further experimental controls, such as nanoparticle comparisons or direct mRNA administration, should also be considered.

Acknowledgements

This work was supported by the Science and Technology Bureau of Danyang under Grant (SSF202109), Jiangsu, China.

Disclosure of conflict of interest

None.

Address correspondence to: Hao Xu, The People's Hospital of Danyang, Affiliated Danyang Hospital of Nantong University, No. 2 Xinmin West Road, Danyang 212300, Jiangsu, China. E-mail: XHresp@163.com

References

[1] Barta JA, Powell CA and Wisnivesky JP. Global epidemiology of lung cancer. Ann Glob Health 2019; 85: 8.

[2] Ju W, Zheng R, Zhang S, Zeng H, Sun K, Wang S, Chen R, Li L, Wei W and He J. Cancer statistics in Chinese older people, 2022: current burden, time trends, and comparisons with the US, Japan, and the Republic of Korea. Sci China Life Sci 2023; 66: 1079-1091.

[3] Siegel RL, Miller KD, Fuchs HE and Jemal A. Cancer statistics, 2022. CA Cancer J Clin 2022; 72: 7-33.

[4] Kratzer TB, Bandi P, Freedman ND, Smith RA, Travis WD, Jemal A and Siegel RL. Lung cancer

statistics, 2023. Cancer 2024; 130: 1330-1348.
[5] Siegel RL, Miller KD, Wagle NS and Jemal A. Cancer statistics, 2023. CA Cancer J Clin 2023; 73: 17-48.
[6] Nandwani A, Rathore S and Datta M. LncRNAs in cancer: regulatory and therapeutic implications. Cancer Lett 2021; 501: 162-171.
[7] Abdi E, Latifi-Navid S, Panahi A and Latifi-Navid H. LncRNA polymorphisms and lung cancer risk. Per Med 2023; 20: 511-522.
[8] Fu J, Yu L, Yan H, Tang S, Wang Z, Dai T, Chen H, Zhang S, Hu H, Liu T, Tang S, He R and Zhou H. LncRNAs in non-small cell lung cancer: novel diagnostic and prognostic biomarkers. Front Mol Biosci 2023; 10: 1297198.
[9] Pan J, Fang S, Tian H, Zhou C, Zhao X, Tian H, He J, Shen W, Meng X, Jin X and Gong Z. lncRNA JPX/miR-33a-5p/Twist1 axis regulates tumorigenesis and metastasis of lung cancer by activating Wnt/beta-catenin signaling. Mol Cancer 2020; 19: 9.
[10] Zhao Y, Feng C, Li Y, Ma Y and Cai R. LncRNA H19 promotes lung cancer proliferation and metastasis by inhibiting miR-200a function. Mol Cell Biochem 2019; 460: 1-8.
[11] Feng C, Zhao Y, Li Y, Zhang T, Ma Y and Liu Y. LncRNA MALAT1 promotes lung cancer proliferation and gefitinib resistance by acting as a miR-200a sponge. Arch Bronconeumol (Engl Ed) 2019; 55: 627-633.
[12] Yang J, Qiu Q, Qian X, Yi J, Jiao Y, Yu M, Li X, Li J, Mi C, Zhang J, Lu B, Chen E, Liu P and Lu Y. Long noncoding RNA LCAT1 functions as a ceRNA to regulate RAC1 function by sponging miR-4715-5p in lung cancer. Mol Cancer 2019; 18: 171.
[13] Wei W, Zhao X, Zhu J, Zhang L, Chen Y, Zhang B, Li Y, Wang M, Zhang Z and Wang C. lncRNA-u50535 promotes the progression of lung cancer by activating CCL20/ERK signaling. Oncol Rep 2019; 42: 1946-1956.
[14] Acha-Sagredo A, Uko B, Pantazi P, Bediaga NG, Moschandrea C, Rainbow L, Marcus MW, Davies MPA, Field JK and Liloglou T. Long noncoding RNA dysregulation is a frequent event in non-small cell lung carcinoma pathogenesis. Br J Cancer 2020; 122: 1050-1058.
[15] Hu Z, Zhu L, Zhang Y and Chen B. N6-methyladenosine-induced SVIL antisense RNA 1 restrains lung adenocarcinoma cell proliferation by destabilizing E2F1. Bioengineered 2022; 13: 3093-3107.
[16] Minciacchi VR, Freeman MR and Di Vizio D. Extracellular vesicles in cancer: exosomes, microvesicles and the emerging role of large oncosomes. Semin Cell Dev Biol 2015; 40: 41-51.
[17] Thery C, Zitvogel L and Amigorena S. Exosomes: composition, biogenesis and function. Nat Rev Immunol 2002; 2: 569-579.
[18] Zhang Y, Liu Y, Liu H and Tang WH. Exosomes: biogenesis, biologic function and clinical potential. Cell Biosci 2019; 9: 19.
[19] Dzialo E, Rudnik M, Koning RI, Czepiel M, Tkacz K, Baj-Krzyworzeka M, Distler O, Siedlar M, Kania G and Blyszczuk P. WNT3a and WNT5a transported by exosomes activate WNT signaling pathways in human cardiac fibroblasts. Int J Mol Sci 2019; 20: 1436.
[20] Li Y, Zheng Q, Bao C, Li S, Guo W, Zhao J, Chen D, Gu J, He X and Huang S. Circular RNA is enriched and stable in exosomes: a promising biomarker for cancer diagnosis. Cell Res 2015; 25: 981-984.
[21] Mao Q, Liang XL, Zhang CL, Pang YH and Lu YX. LncRNA KLF3-AS1 in human mesenchymal stem cell-derived exosomes ameliorates pyroptosis of cardiomyocytes and myocardial infarction through miR-138-5p/Sirt1 axis. Stem Cell Res Ther 2019; 10: 393.
[22] Valadi H, Ekstrom K, Bossios A, Sjostrand M, Lee JJ and Lotvall JO. Exosome-mediated transfer of mRNAs and microRNAs is a novel mechanism of genetic exchange between cells. Nat Cell Biol 2007; 9: 654-659.
[23] Wang S, Wang J, Wei W and Ma G. Exosomes: the indispensable messenger in tumor pathogenesis and the rising star in antitumor applications. Adv Biosyst 2019; 3: e1900008.
[24] Gilligan KE and Dwyer RM. Engineering exosomes for cancer therapy. Int J Mol Sci 2017; 18: 1122.
[25] Vakhshiteh F, Rahmani S, Ostad SN, Madjd Z, Dinarvand R and Atyabi F. Exosomes derived from miR-34a-overexpressing mesenchymal stem cells inhibit in vitro tumor growth: a new approach for drug delivery. Life Sci 2021; 266: 118871.
[26] Kim H, Kim EH, Kwak G, Chi SG, Kim SH and Yang Y. Exosomes: cell-derived nanoplatforms for the delivery of cancer therapeutics. Int J Mol Sci 2020; 22: 14.
[27] Terstappen GC, Meyer AH, Bell RD and Zhang W. Strategies for delivering therapeutics across the blood-brain barrier. Nat Rev Drug Discov 2021; 20: 362-383.
[28] Yang T, Martin P, Fogarty B, Brown A, Schurman K, Phipps R, Yin VP, Lockman P and Bai S. Exosome delivered anticancer drugs across the blood-brain barrier for brain cancer therapy in Danio rerio. Pharm Res 2015; 32: 2003-2014.
[29] Batrakova EV and Kim MS. Using exosomes, naturally-equipped nanocarriers, for drug delivery. J Control Release 2015; 219: 396-405.

[30] Li YJ, Wu JY, Liu J, Xu W, Qiu X, Huang S, Hu XB and Xiang DX. Artificial exosomes for translational nanomedicine. J Nanobiotechnology 2021; 19: 242.
[31] Liang G, Kan S, Zhu Y, Feng S, Feng W and Gao S. Engineered exosome-mediated delivery of functionally active miR-26a and its enhanced suppression effect in HepG2 cells. Int J Nanomedicine 2018; 13: 585-599.
[32] Liang G, Zhu Y, Ali DJ, Tian T, Xu H, Si K, Sun B, Chen B and Xiao Z. Engineered exosomes for targeted co-delivery of miR-21 inhibitor and chemotherapeutics to reverse drug resistance in colon cancer. J Nanobiotechnology 2020; 18: 10.
[33] Li B, Yang J, Wang R, Li J, Li X, Zhou X, Qiu S, Weng R, Wu Z, Tang C and Li P. Delivery of vascular endothelial growth factor (VEGFC) via engineered exosomes improves lymphedema. Ann Transl Med 2020; 8: 1498.
[34] Ye Y, Zhang X, Xie F, Xu B, Xie P, Yang T, Shi Q, Zhang CY, Zhang Y, Chen J, Jiang X and Li J. An engineered exosome for delivering sgRNA:Cas9 ribonucleoprotein complex and genome editing in recipient cells. Biomater Sci 2020; 8: 2966-2976.
[35] Mentkowski KI and Lang JK. Exosomes engineered to express a cardiomyocyte binding peptide demonstrate improved cardiac retention in vivo. Sci Rep 2019; 9: 10041.
[36] Bai J, Duan J, Liu R, Du Y, Luo Q, Cui Y, Su Z, Xu J, Xie Y and Lu W. Engineered targeting tLyp-1 exosomes as gene therapy vectors for efficient delivery of siRNA into lung cancer cells. Asian J Pharm Sci 2020; 15: 461-471.
[37] Nie H, Xie X, Zhang D, Zhou Y, Li B, Li F, Li F, Cheng Y, Mei H, Meng H and Jia L. Use of lung-specific exosomes for miRNA-126 delivery in non-small cell lung cancer. Nanoscale 2020; 12: 877-887.
[38] Guo L, Ding L and Tang J. Identification of a competing endogenous RNA axis "SVIL-AS1/miR-103a/ICE1" associated with chemoresistance in lung adenocarcinoma by comprehensive bioinformatics analysis. Cancer Med 2021; 10: 6022-6034.